

# Generalized High-order Phase Function for Parameter Estimation of Polynomial Phase Signal

*Pu Wang, Igor Djurović, and Jianyu Yang*

*Abstract*— The high-order phase function (HPF) has been introduced recently to estimate the parameters of a polynomial phase signal (PPS). In this paper, we generalize the standard HPF by introducing multiple time instants. Thus, the standard HPF can be treated as a special example of the generalized HPF with identical time instants. We propose procedure for finding time instants minimizing the mean squared error (MSE). The proposed method achieves better performances than the high-order ambiguity function (HAF) and polynomial Wigner-Ville distribution (PWVD). The theoretical analysis as well as the Monte-Carlo simulations verify the advantages such as lower MSE and lower SNR threshold for the PPS.

## I. INTRODUCTION

The polynomial phase structure has been widely used to model non-stationary signal appearing in radar (e.g., pulse-Doppler radar, SAR and ISAR), sonar, communications, biomedicine, seismic analysis, animal sounds modeling and passive acoustic applications [1–4]. For example, in radar, the output of the matched filter can be well approximated by a polynomial of a finite order within a closed interval, according to the Weierstrass theorem.

The parameter estimation of polynomial phase signal (PPS) with constant amplitude has received much attention for the last two decades. The maximum likelihood estimation (MLE) [5], which is asymptotically efficient, requires high computational load for multi-parameter estimation. In addition, the cost function in the MLE could have poor numerical properties due to many local maxima. A number of simpler approaches have been presented to reduce the computational complex-

ity. The rank reduction technique for linear FM signals (the second-order PPS) was extended by Peleg and co-workers, to deal with higher-order PPS. This approach was then referred to as the discrete polynomial transform (DPT) or the high-order ambiguity function (HAF) [3, 6, 7]. The HAF-based approach employs iterative finite differences of the phase to obtain a sinusoid at a certain frequency directly proportional to the highest-order phase parameter. This parameter can then be estimated by using a number of spectral estimation techniques. Meanwhile, advances in the time-frequency (TF) distribution for the generic non-stationary signal can be applied to analyze the PPS. Typically, the polynomial Wigner-Ville distribution (PWVD) was proposed for the PPS with arbitrary order in a way analogous to the WVD for the linear FM signal [8]. The PWVD transforms the signal to ensure a delta function around the instantaneous frequency (IF) of the signal in the TF domain. Besides the HAF and PWVD, the instantaneous frequency rate (IFR) estimator has been recently developed by O’Shea in [9] and [10]. While the IF is defined as the first-order derivative of the phase, the IFR can be considered as the second-order derivative of the phase. In analogy to the PWVD, the high-order phase function (HPF) [10] was proposed to reveal the variation of the IFR with respect to time. Specifically, in the case of the quadratic FM signal (the third-order PPS), the second-order HPF is reduced to the cubic phase function (CPF), which provides a lower SNR threshold at SNR = -2 dB when the number of samples is 257 [10].

Here, we generalize the standard HPF by relaxing the constraint on identical time in-

starts. The additional time redundancy allows us to find a nonlinear transform with lower order for the PPS. Hence, the proposed method offers some advantages compared with conventional methods. The theoretical results via the first-order perturbation principle show lower MSE and lower SNR threshold for the proposed method compared with the HAF and PWVD. In particular, for a fourth-order PPS, the proposed method provides a SNR threshold as low as 3 dB, which is 4 and 7 dB smaller than the PWVD and HAF, respectively. In essence, the CPF, the HPF and the generalized CPF in [14] can all be interpreted as special cases of the method proposed in this paper. In other words, the proposed method could inherit the conventional advantages of the HPF in certain cases (i.e., the low order of nonlinearity of the CPF) and it improves the performance of the HPF in other cases (i.e., lower MSE of the algorithm in [14]).

The rest of this paper is organized as follows. Section II first briefly reviews the HAF and PWVD. Then, we establish lag-coefficient equations for the standard HPF. In Section III, the generalized high-order phase function (GHPF) is defined and corresponding properties are provided. To gain insight into the GHPF, we present several specific examples. Section IV provides an asymptotic closed-form expression of the MSE for the GHPF-based estimates via the first-order perturbation principle. The theoretical results are identified using the Monte-Carlo simulations in Section V. Finally, conclusions are provided in Section VI.

## II. HIGH-ORDER PHASE FUNCTION

The signal considered in this paper is modeled as follows:

$$\begin{aligned} x(t) &= s(t) + v(t) = A \exp \{j\phi(t)\} + v(t) \\ &= A \exp \left\{ j \sum_{i=0}^p a_i t^i \right\} + v(t), \end{aligned} \quad (1)$$

where  $A$  is the amplitude,  $\phi(t)$  is the  $p$ th-order polynomial phase,  $\{a_i\}_{i=0}^p$  are unknown phase parameters,  $v(t)$  is white Gaussian noise with zero mean and variance  $\sigma^2$ , and  $t \in [-T/2, T/2]$ .

For the PPS defined in (1), a number of techniques can be applied to estimate the parameters, i.e., the HAF [3], PWVD [8] and HPF [10]. The phase differentiation in the HAF is performed  $(p-1)$  times. The highest order parameter  $a_p$  is estimated based on obtained sinusoid. The order of non-linearity in this transform is  $2^{(p-1)}$ . The lag-coefficients of the PWVD are selected in such a manner that the PWVD is concentrated around the IF of (1) (see (5) and (6) in [8]). For example, for a quadratic FM,  $p=3$ , or for a cubic FM signal,  $p=4$ , [8] gave two solutions regarding the lag-coefficients: (1)  $d_1 = d_2 \approx 0.675, d_3 \approx -0.85$  and (2)  $d_1 \approx 0.62, d_2 \approx 0.75, d_3 \approx -0.87$ . In both cases, the PWVD contains the sixth-order nonlinearity.

The  $q$ th-order HPF can be considered as the output of the quadratic phase filter with the input (nonlinear kernel):  $K_q(t; \mathbf{d}) = \prod_{l=1}^{q/2} [s(\mathbf{t} + \mathbf{d}_l \boldsymbol{\tau}) s(\mathbf{t} - \mathbf{d}_l \boldsymbol{\tau})]^{r_l}$ , where  $\mathbf{d}$  is the set of lag-coefficients,  $\mathbf{d} = \{\mathbf{d}_1, \mathbf{d}_2, \dots, \mathbf{d}_{q/2}\}$  and the symbol  $[\cdot]^{r_l}$  indicates the conjugation of  $[\cdot]$  if  $r_l = -1$  and  $[\cdot]$  if  $r_l = 1$ ; or, equivalently [10],

$$W_q(t, \Omega) = \int_{-\infty}^{+\infty} K_q(t; \mathbf{d}) e^{-j\Omega \boldsymbol{\tau}^2} \mathbf{d} \boldsymbol{\tau}, \quad (2)$$

where  $\Omega$  denotes the IFR spectrum. With  $q=2, d_1=1$  and  $r_l=1$  in (2), the  $W_2(t, \Omega)$  turns into the CPF in [10]. To concentrate the energy along the IFR of the signal, we give the following proposition without proof<sup>1</sup>.

*Proposition 1:* For a  $p$ th-order PPS, the lag-coefficients of the HPF should be chosen from the real solutions of the following equations:

$$\begin{aligned} \sum_{l=0}^{q/2} r_l d_l^2 &= 1, \\ \sum_{l=0}^{q/2} r_l d_l^m &= 0, \text{ for even } m: 4 \leq m \leq p. \end{aligned}$$

Provided that the lag-coefficients satisfy the *Proposition 1*, the kernel  $K_q(t; \mathbf{d})$  of the HPF

<sup>1</sup>All related derivations are available at <http://personal.stevens.edu/~pwan/g4/index.htm>

is shown to be  $K_q(t; \mathbf{d}) = \mathbf{A}^q \mathbf{e}^{j[\tau^2 \text{IFR}(t) + \zeta]}$ , while the corresponding  $q$ th-order HPF can be expressed as  $|W_q(t, \Omega)| = A^q \sqrt{\frac{\pi}{|\text{IFR}(t) - \Omega|}}$ , with the help of the following equations [11]

$$\int_{-\infty}^{\infty} \sin ax^2 dx = \int_{-\infty}^{\infty} \cos ax^2 dx = \sqrt{\frac{\pi}{2a}}. \quad (3)$$

The above results suggest a HPF-based estimation algorithm for a PPS with a known order  $p$ : 1) for a specified iteration index  $\ell$  (initiate  $\ell = 1$ ), only one time instant  $t_\ell$  is determined and the corresponding IFR( $t_\ell$ ) is obtained by directly searching the maximum of  $|W_q(t, \Omega)|$  over the set of  $\Omega$  values; 2) repeat the iteration step until  $\ell = p - 1$ . In other words, we select  $p - 1$  values of IFR at ( $p - 1$ ) time instants and then simultaneously solve the set of  $p - 1$  equations to find the estimates, i.e.,

$$\begin{pmatrix} \hat{a}_2 \\ \vdots \\ \hat{a}_p \end{pmatrix} = \begin{pmatrix} 2 & \cdots & p(p-1)t_1^{p-2} \\ \vdots & \ddots & \vdots \\ 2 & \cdots & p(p-1)t_{p-1}^{p-2} \end{pmatrix}^{-1} \times \begin{pmatrix} \text{IFR}(t_1) \\ \vdots \\ \text{IFR}(t_{p-1}) \end{pmatrix}.$$

The rest phase parameters, i.e.,  $a_1$  and  $a_0$ , can be estimated using conventional frequency estimation techniques by dechirping the observed signal with the obtained estimates.

The analysis of the estimation accuracy is performed only for the quadratic FM signal [9, 10]. In general,  $p - 1$  time instants should be jointly chosen to minimize the MSE of the estimates. For example, for the quadratic FM signal with  $p = 3$ , two time instants,  $n = 0$  and  $n = 0.11N$ , are jointly selected to lower the MSE of both  $a_2$  and  $a_3$  estimates, where  $N$  is the number of samples [10].

### III. GENERALIZED HIGH-ORDER PHASE FUNCTION

From the HPF-based method, it is apparent that the time instant is constrained by using only one time instant  $t_\ell$  in one iteration

step. To relax this constraint, we generalize the HPF by involving multiple time instants  $\mathbf{t}_\ell$  in one iteration step, where  $\mathbf{t}_\ell$  includes  $q/2$  time instants, i.e.,  $\mathbf{t}_\ell = \{\mathbf{t}_{\ell,1}, \dots, \mathbf{t}_{\ell,q/2}\}$ . The multiple time instants may be different or identical to each other, depending on the problem at hand. In particular, the GHPF employing identical time instants reduces to the standard HPF. Correspondingly, the IFR is extended to the generalized IFR which admits the time sets  $\mathbf{t}_\ell$ .

#### A. Definition

By introducing multiple time instants, the GHPF can be defined as the output of the quadratic phase filter with input (nonlinear kernel)  $K_q^G(\mathbf{t}; \mathbf{d}) = \prod_{l=1}^{q/2} [s(\mathbf{t}_l + \mathbf{d}_l \tau) s(\mathbf{t}_l - \mathbf{d}_l \tau)]^{r_l}$ , or, equivalently,

$$S_q(\mathbf{t}, \omega) = \int_{-\infty}^{+\infty} \mathbf{K}_q^G(\mathbf{t}; \mathbf{d}) e^{-j\omega \tau^2} d\tau, \quad (4)$$

where  $\mathbf{t}$  denotes the set of  $t_1, t_2, \dots, t_{q/2}$ , and  $\omega$  represents the generalized IFR spectrum.

Correspondingly, we generalize the IFR which admits multiple time instants:

$$\omega(\mathbf{t}) = \sum_{i=2}^p \mathbf{i}(i-1) \mathbf{a}_i \sum_{l=1}^{q/2} r_l d_l^2 t_l^{i-2}. \quad (5)$$

Compared to the IFR, the generalized IFR replaces the time instant  $t$  with a time sets weighted by lag-coefficients  $\sum_{l=1}^{q/2} r_l d_l^2 t_l^{i-2}$ . By setting  $t_1 = t_2 = \dots = t_{q/2}$ , the generalized IFR reduces to the standard IFR with a scale factor  $\sum_{l=1}^{q/2} r_l d_l^2$ . In order to represent the  $p$ th-order PPS as a delta function around the generalized IFR, it is required that the lag-coefficients and time instants should satisfy the following proposition.

*Proposition 2:* Given a  $p$ th-order PPS, the lag-coefficients for the GHPF should be chosen from the real solutions of the following equations:

$$\sum_{l=1}^{q/2} r_l d_l^m t_l^{i-m} = 0, \quad \text{for even value of } m, \text{ where } 4 \leq m \leq p, \text{ and } m \leq i \leq p.$$

TABLE I  
THE ORDER OF NONLINEARITY FOR DIFFERENT  $p$ 's

$p$	2	3	4	5
HAF	2	4	8	16
PWVD	2	6	6	8
GHPF	2	2	4	6

Given that the lag-coefficients and time instants satisfy the *Proposition 2*, the GHPF can be computed with the help of (3) as  $|S_q(\mathbf{t}, \omega)| = \mathbf{A}^q \sqrt{\frac{\pi}{|\omega(\mathbf{t}) - \omega|}}$ . The point of extreme is the generalized IFR of a  $p$ th-order PPS.

*Remark 1:* For a  $p$ th-order PPS, the best GHPF, under the terms of MSE or SNR threshold, performs at least as well as the best standard HPF. Obviously, the best standard HPF or the best GHPF must be one of the solutions of the *Proposition 1* or the *Proposition 2*, respectively. Moreover, the solutions of *Proposition 1* are always solutions of *Proposition 2* for identical time instants. Therefore, the best GHPF can always duplicate when the best solutions in both cases are identical, or outperform the best standard HPF otherwise.

*Remark 2:* For a  $p$ th-order PPS, there always exists a GHPF with nonlinearity order less than or equal to the order of the HAF and PWVD. We first examine this property by enumerating a number of cases that mostly occur, i.e., the PPS with  $p \leq 5$  that is adequate to model the most frequently occurring signals in practical applications [1–4]. As shown in Table I, the order of nonlinear transform in HAF for a  $p$ th-order PPS is  $2^{p-1}$  [3]. It is shown that the HAF has much higher order of nonlinearity than the PWVD and the GHPF, when the order of PPS is higher. Meanwhile, the order of nonlinearity in the PWVD is generally larger than the GHPF, except the second-order case. For a larger  $p$ , this property can be proven in a similar manner. Therefore, we expect that the GHPF provides a lower order nonlinear transform than the HAF and PWVD for the PPS.

### B. Estimation Algorithm

The parameter estimation of a PPS using the GHPF can be performed similarly to the procedure of the HPF in Section II. For a PPS with a known order  $p$ , the estimation procedure can be specified as follows:

- Initialize the iteration index as  $\ell = 1$ , and search the grid maximizing the GHPF for a given  $\mathbf{t}_\ell$ ;
- Repeat the above procedure and set  $\ell = \ell + 1$  until  $\ell = p - 1$ ;
- Estimate the corresponding parameters by simultaneously solving the resulting equations;
- Demodulate the observed signal with the estimated parameters:

$$x(t) = x(t)e^{-j(\hat{a}_p t^p + \dots + \hat{a}_2 t^2)};$$

- Estimate the remaining parameters, i.e.,  $a_1$ ,  $a_0$  and  $A$  by using spectral analysis techniques.

In the presence of multicomponent signals, the GHPF has cross-terms due to inherent nonlinear transform. According to *Remark 2*, the GHPF may produce less cross-terms because of its lower order of nonlinearity than the HAF and PWVD. Furthermore, motivated by the PHAF [12] which utilizes additional lag redundancy in the standard HAF for multicomponent PPS, the GHPF could have extra performance gain for multicomponent signals by properly designing. For multicomponent second- and third-order PPSs, two algorithms based on the GHPF are suggested in [13] and [14] by adopting a similar idea of PHAF and the spectral scaling technique.

### C. Examples

From Table I, it is shown that, for the third-, fourth-, and fifth-order PPSs, the GHPF has the lowest order of nonlinearity. This is the important property since it assures better performance of the corresponding estimator. In this part, we specify two examples of  $p = 3$  and  $p = 4$  and present the relationship between the GHPF and the proposed methods in [10] and [14].

Specifically, the third- and fourth-order PPSs can be found in many practical applications. While the third-order PPS can be detected in the passive radar surveillance and

modeling of echoes from bats [10], the fourth-order PPS can be found in the underwater field, i.e., the receiving signal is a fourth-order PPS if the transmitter sends a linear FM signal to detect a moving source [15]. In addition, signals produced by underwater mammals and signals from Diesel engines can be modeled as the fourth-order PPS [15].

For a third-order PPS, two GHPF-based methods can be used to estimate the parameters. The first one is the CPF, which is a member of the second-order GHPF with  $d_1 = 1$  and  $r_1 = 1$  [10]:

$$S_2(t, \omega) = \int_{-\infty}^{+\infty} s(t + \tau)s(t - \tau)e^{-j\omega\tau^2} d\tau. \quad (6)$$

The order of inherent nonlinearity is only 2 and hence the SNR threshold is much lower than the HAF and the PWVD. See [10] for the detail. The other method is the generalized CPF, which is an example of the fourth-order GHPF with coefficient  $t_1 = -t_2 = t$ ,  $d_1 = d_2 = 1$  and  $r_1 = -r_2 = 1$  [14]:

$$S_4(t, -t, \omega) = \int_{-\infty}^{+\infty} s(t + \tau)s(t - \tau) \times s^*(-t + \tau)s^*(-t - \tau)e^{-j\omega\tau^2} d\tau. \quad (7)$$

In [14], the above estimator exhibits lower MSE than the CPF and HAF at high SNR.

For a fourth-order PPS, we could find a fourth-order GHPF to estimate the parameters. This fourth-order GHPF can be specified with lag coefficients  $d_1 = d_2 = 1$  and  $r_1 = -r_2 = 1$ :

$$S_4(t_1, t_2, \omega) = \int_{-\infty}^{+\infty} s(t_1 + \tau)s(t_1 - \tau) \times s^*(t_2 + \tau)s^*(t_2 - \tau)e^{-j\omega\tau^2} d\tau. \quad (8)$$

As a result of low order of nonlinearity, the fourth-order GHPF provides a lower SNR threshold than the HAF and PWVD as shown in Section V. To the best of our knowledge the GHPF has the lowest nonlinearity for the fourth-order PPS.

#### IV. STATISTICAL ANALYSIS

The considered estimators are compared here in terms of the asymptotic MSE and SNR threshold. The asymptotic MSE is determined by using the first-order perturbation method [16], which is assumed valid for high SNR and for sufficiently large discrete samples. The perturbation method is described in Appendix II, where it is applied to the second-, third- and fourth-order cases. For simplicity, theoretical results are listed only for the  $p$ th- or  $(p - 1)$ st-order phase parameters. Herein, in the first-order perturbation analysis, the continuous notation will be changed to corresponding discrete notation, i.e., the integral in (8) is replaced with corresponding summation.

As the main results we have found that the proposed estimator is asymptotically unbiased. The asymptotic MSEs are presented in Appendix. To compare the derived asymptotic MSE with corresponding CRB [17], we use the asymptotic efficiency ratio (AER),  $\kappa$ , defined as the ratio between the asymptotic MSE and corresponding CRB. In particular, the AER in the second-order case is

$$\kappa_{a_2} = 1 + \frac{0.5}{\text{SNR}}.$$

For the third-order PPS, the AERs are

$$\begin{aligned} \kappa_{a_3}^e &= 1.1307 + \frac{2.0212}{\text{SNR}}, \\ \kappa_{a_3}^c &= 1.4557 + \frac{1.3247}{\text{SNR}}, \\ \kappa_{a_2}^c &= 1 + \frac{0.5}{\text{SNR}}. \end{aligned}$$

where superscripts  $c$  and  $e$  denote the CPF and the generalized CPF in (7), respectively. Finally, the AERs for the fourth-order PPS are

$$\begin{aligned} \kappa_{a_4} &= 1.8786 + \frac{3.9536}{\text{SNR}}, \\ \kappa_{a_3} &= 1.1307 + \frac{2.0212}{\text{SNR}}. \end{aligned}$$

It is obvious that the GHPF provides lower MSE than the HAF-based method (Table I in [7] lists the  $[\text{ARE}]^{0.5}$  for the HAF). To compare the proposed method with the PWVD, we

TABLE II  
THE SNR THRESHOLD FOR DIFFERENT  $p$ 's

$p$	2	3	4	5
$\gamma_p^{\text{HAF}}$ (dB)	-3	3	10	16
$\gamma_p^{\text{PWVD}}$ (dB)	-3*	7*	7*	11*
$\gamma_p^{\text{GHPF}}$ (dB)	-3	-3	3	5*

would like to employ the Monte-Carlo simulations, since the theoretical result is not available for the PWVD-based method that is originally proposed for the IF estimate.

On the other hand, it is meaningful to compare the performance in terms of the SNR threshold with respect to the HAF and PWVD. In general, nonlinear estimators always exhibit the threshold effect [18]. That is, at the SNR below this threshold, the first-order perturbation is not valid due to the assumption of high SNR. One possible way to explicitly approximate the SNR threshold is presented in [7]. Following the main derivations in [7], we define here the SNR threshold  $\gamma_p$  as

$$\gamma_p = \min \{10 \log_{10} \text{SNR}_t^\rho\}, \quad (9)$$

where  $\text{SNR}_t^\rho$  satisfies

$$\kappa_{a_\rho}(\text{SNR} = \text{SNR}_t^\rho) = 2\kappa_{a_\rho}(\text{SNR} = \infty), \quad (10)$$

and  $1 \leq \rho \leq p$ . As an example of  $p = 4$ ,  $\text{SNR}_t^4 \approx 2.11$ ,  $\text{SNR}_t^3 \approx 1.79$ , and inserting 1.79 to (9) approximates the threshold at  $\text{SNR} \approx 2.53$  dB. Table II presents the round-up SNR thresholds of the HAF, the PWVD and the GHPF for a PPS with  $p \leq 5$ , where \* denotes that the threshold obtained in simulations.

As stated above, the theoretical results on asymptotic efficiency ratio of the PWVD is not available, and hence it is difficult to explicitly express its SNR threshold using (9). This problem can be considered in an alternative way. At low SNR (i.e., below the SNR threshold), the asymptotic MSE of the PWVD-based estimator contains higher power of the SNR than the GHPF [7]. In particular, for  $p = 4$ ,

the asymptotic MSEs of the GHPF should vary in proportion to  $\text{SNR}^{-4}$  (see Sect. III and IV in [7] and Sect. III in [10]), whereas the MSEs of the PWVD and HAF vary with  $\text{SNR}^{-6}$  and  $\text{SNR}^{-8}$ , respectively. Therefore, it can be assumed that the SNR threshold of the PWVD falls between the thresholds of the HAF at  $\text{SNR} \approx 10$  dB and that of the GHPF at  $\text{SNR} \approx 3$  dB. Indeed, the Monte-Carlo simulation shows a threshold at  $\text{SNR} \approx 7$  dB of the PWVD for  $p = 4$ .

## V. NUMERICAL SIMULATIONS

To evaluate the performance of the GHPF-based estimator, we present the Monte-Carlo simulation results in terms of MSE as a function of SNR for the fourth- and fifth-order PPSs. For a third-order PPS, the performance corresponding to the CPF and the generalized CPF can be found in [10] and [14]. Meanwhile, the performance of the HAF and PWVD will be demonstrated and compared with the GHPF. The simulated MSEs are computed with 200 runs at each SNR and compared with corresponding CRB. Signal embedded in the additive, complex, white Gaussian noise with zero mean is considered. The SNR is incremented in 1-dB interval between -5 and 20 dB, the sampling interval is 1, and the number of samples is  $N = 257$ .

In Figs. 1 and 2, the performance of the considered methods in estimation of  $a_3$  and  $a_4$  parameters for a fourth-order PPS is presented. The parameters of the fourth-order PPS are chosen to be  $A = 1$ ,  $a_4 = 0.4\pi 10^{-8}$ ,  $a_3 = 0.2\pi 10^{-5}$ ,  $a_2 = -0.2\pi 10^{-3}$ ,  $a_1 = 0.4\pi$ , and  $a_0 = 0$ . Specifically, the time instants in the GHPF are  $(0.229N, -0.229N)$  and  $(0.276N, -0.098N)$ , whereas the HAF employs the lag set as  $(N/2P)$  with  $P = 4$  for the  $a_4$  estimate and  $P = 3$  for the  $a_3$  estimate, and the PWVD uses the following time sets:  $(-3/8N, -1/4N, 0, 1/4N)$ . Note that, in this case, the PWVD is implemented with the eighth-order interpolation due to its lag-coefficients, whereas the GHPF and HAF are used without interpolation. As the figures shown, the GHPF provides marginally lower MSE than the HAF and PWVD with respect to the CRB. Furthermore, the SNR threshold

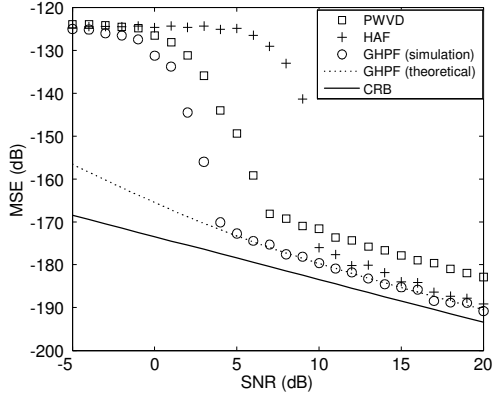


Fig. 1. MSEs of the  $a_4$  estimate using the HAF, PWVD and GHPF for a fourth-order PPS

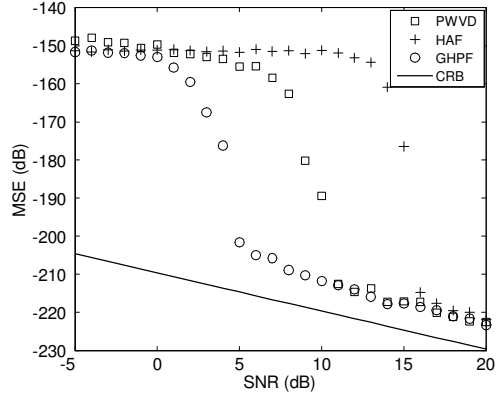


Fig. 3. MSEs of the  $a_5$  estimate using the HAF, PWVD and GHPF for a fifth-order PPS

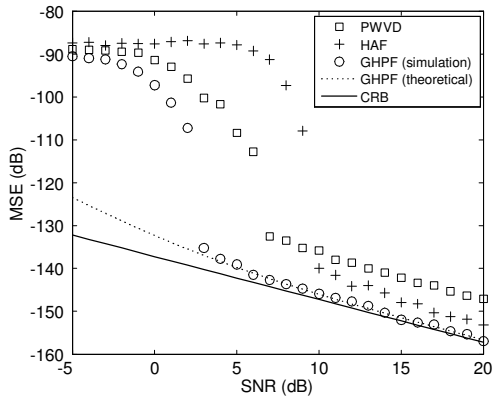


Fig. 2. MSEs of the  $a_3$  estimate using the HAF, PWVD and GHPF for a fourth-order PPS

for the GHPF is about 3 dB, approaching the SNR threshold in Table II. The threshold in the GHPF is smaller for 4 dB and 7 dB than the corresponding thresholds in the PWVD and HAF. For the SNR above this threshold, the theoretical MSE is accurate approximation of the simulated MSE.

Fig. 3 presents the simulation results for a fifth-order PPS. The corresponding parameters are chosen to be  $A = 1$ ,  $a_5 = 0.4\pi 10^{-10}$ ,  $a_4 = 0.4\pi 10^{-8}$ ,  $a_3 = \pi 10^{-5}$ ,  $a_2 = -\pi 10^{-3}$ ,  $a_1 = 0.2\pi$ , and  $a_0 = 0$ . The lag-coefficients of the sixth-order GHPF are chosen as  $\mathbf{d} = (0.707, 0.760, 0.527)$ ,  $r_1 = r_3 = -r_2 = 1$ , and  $t_1 = 2t_2 = -t_3$ . Specifically, four time instants of  $t_1$  in discrete time are

$(-N/8, -N/4, N/8, N/4)$ , whereas the HAF employs the lag set as  $(N/2P)$  with  $P = 5$  and the PWVD uses the following time sets:  $(-3/8N, -1/4N, 0, 1/4N, 3/8N)$ . Due to the lag-coefficients, both GHPF and PWVD are implemented with the eighth-order interpolation, while the HAF is evaluated without interpolation. As shown in Fig. 3, the SNR thresholds of the PWVD and HAF are 11 and 16 dB, which are 6 and 11 dB higher than that of the sixth-order GHPF. Marginally, the MSEs of the GHPF are lower than the HAF and PWVD, especially at the SNR below 11 dB.

## VI. CONCLUSION

The GHPF has been presented by introducing multiple time instants. Key properties of the GHPF are given. Moreover, we have elaborated the cases of  $p = 3$  and  $p = 4$  to illustrate that the GHPF can employ lower order nonlinearity than other considered transforms. The statistical analysis via the first-order perturbation principle and the Monte-Carlo simulation present the advantages with respect to conventional methods in terms of lower MSE and smaller SNR threshold.

## APPENDIX

### I. THEORETICAL MSE OF THE ESTIMATES

The basic principle of the first-order perturbation method is shown as follows [16]. As

sume that  $g_N(\omega)$  is a complex function depending on a real variable  $\omega$  and on an integer  $N$ , with a global maximum at  $\omega = \omega_0$ . A random function  $\delta g_N(\omega)$  moves the global maximum for  $\delta\omega$ . The first-order approximation for  $\delta\omega$  is

$$\delta\omega \approx -\frac{\beta}{\alpha} \tag{11}$$

where

$$\alpha = 2\Re \left\{ g_N(\omega_0) \frac{\partial^2 g_N^*(\omega_0)}{\partial \omega^2} + \frac{\partial g_N(\omega_0)}{\partial \omega} \frac{\partial g_N^*(\omega_0)}{\partial \omega} \right\}, \tag{12}$$

and

$$\beta = 2\Re \left\{ g_N(\omega_0) \frac{\partial \delta g_N^*(\omega_0)}{\partial \omega} + \frac{\partial g_N(\omega_0)}{\partial \omega} \delta g_N^*(\omega_0) \right\}, \tag{13}$$

where  $\Re(\cdot)$  represents the real part of  $(\cdot)$ . The mean-square value of  $\delta\omega$  is given by

$$E\{(\delta\omega)^2\} \approx \frac{E\{\beta^2\}}{\alpha^2}, \tag{14}$$

where  $E\{\cdot\}$  denotes the expectation.

*A. The Second-order PPS*

It can be easy to obtain the asymptotic MSE in the second-order case. For a given SNR defined as  $A^2/\sigma^2$  and  $N$ , the asymptotic MSE for the  $a_2$  estimate minimizes at  $n = 0$ :

$$E\{(\delta a_2)^2\} \approx \frac{90(1 + \frac{1}{2\text{SNR}})}{\text{SNR}N^5}. \tag{15}$$

*B. The Third-order PPS*

For the third-order PPS, two GHPF-based methods are available: the CPF and generalized CPF. For the CPF, the point of global maximum is  $\omega_0 = 2a_2 + 6a_3n$  and the asymptotic MSEs of the  $a_3$  and  $a_2$  estimates are [10]

$$E\{(\delta a_3)^2\} = \frac{2038(1 + \frac{0.91}{\text{SNR}})}{N^7\text{SNR}}, \tag{16}$$

$$E\{(\delta a_2)^2\} = \frac{90(1 + \frac{0.5}{\text{SNR}})}{N^5\text{SNR}}. \tag{17}$$

For the generalized CPF, the global maximum is  $\omega_0 = 12a_3n$  and the asymptotic MSE of the  $a_3$  estimate is [14]

$$E\{(\delta a_3)^2\} = \frac{1583(1 + \frac{1.93}{\text{SNR}})}{N^7\text{SNR}}. \tag{18}$$

Moreover, both estimators are asymptotically unbiased [10], [14].

*C. The Fourth-order PPS*

For a fourth-order PPS, the fourth-order GHPF in (8) is employed. For simplicity of notation, let us define the following variables:  $s_1 = s(n_1 + m), s_2 = s(n_1 - m), s_3 = s(n_2 + m), s_4 = s(n_2 - m), v_1 = v(n_1 + m), v_2 = v(n_1 - m), v_3 = v(n_2 + m)$  and  $v_4 = v(n_2 - m)$ . According to the first-order perturbation method, we approximate a complex function depending on variable  $\omega$  and its perturbation under assumption of high SNR:

$$g_N(\omega) = \sum_{m=0}^{N_1} s_1 s_2 s_3^* s_4^* e^{-j\omega m^2}, \tag{19}$$

$$\delta g_N(\omega) \approx \sum_{m=0}^{N_1} z_{sv}(n_1, n_2, m) e^{-j\omega m^2}, \tag{20}$$

where  $N_1 = N/2 - \max\{|n_1|, |n_2|\}$ , and  $z_{sv}(n_1, n_2, m)$  approximates the interference terms containing not more than two noise factors:

$$\begin{aligned} z_{sv}(n_1, n_2, m) = & \\ & = s_1 s_2 s_3^* v_4^* + s_1 s_2 s_4^* v_3^* + s_1 s_2 v_3^* v_4^* + s_1 s_3^* s_4^* v_2 \\ & + s_1 s_3^* v_2 v_4^* + s_1 s_4^* v_2 v_3^* + s_2 s_3^* s_4^* v_1 \\ & + s_2 s_3^* v_1 v_4^* + s_2 s_4^* v_1 v_3^* + s_3^* s_4^* v_1 v_2. \end{aligned} \tag{21}$$

The functions  $g_N(\omega), \delta g_N(\omega)$ , and their derivatives, evaluated at the global maximum  $\omega_0 = 6[a_3(n_1 - n_2) + 2a_4(n_1^2 - n_2^2)]$ , are given



by

$$\begin{aligned}
 g_N(\omega_0) &\approx A^4 \varphi N_1, \\
 \frac{\partial g_N(\omega_0)}{\partial \omega} &\approx -j A^4 \varphi \frac{N_1^3}{3}, \\
 \frac{\partial^2 g_N(\omega_0)}{\partial \omega^2} &\approx -A^4 \varphi \frac{N_1^5}{5}, \\
 \delta g_N(\omega_0) &\approx \sum_{m=0}^{N_1} z_{sv}(n_1, n_2, m) e^{-j\omega_0 m^2}, \\
 \frac{\partial \delta g_N(\omega_0)}{\partial \omega} &\approx -j \sum_{m=0}^{N_1} m^2 z_{sv}(n_1, n_2, m) e^{-j\omega_0 m^2},
 \end{aligned}$$

where  $\varphi = e^{j \sum_{i=1}^4 a_i (n_1^i - n_2^i)}$ . Using (12) and (13), we derive

$$\alpha \approx \frac{-8A^8 N_1^6}{45}, \tag{22}$$

$$\beta \approx -2A^4 N_1 [\Im\{\Gamma\}], \tag{23}$$

where

$$\Gamma \approx \varphi \sum_{m=0}^{N_1} \left( m^2 - \frac{N_1^2}{3} \right) z_{sv}^*(n_1, n_2, m) e^{j\omega_0 m^2}.$$

The first-order approximation of  $\delta\omega$  using (11) is given as:

$$\delta\omega \approx -\frac{45 \cdot \Im\{\Gamma\}}{4A^4 N_1^5}. \tag{24}$$

Its expectation, which is the first-order approximation of the estimate bias, is approximately zero.

With the following intermediate results,

$$E\{\Gamma\Gamma^*\} \approx (4A^6 \delta^2 + 6A^4 \delta^4) \frac{4N_1^5}{45},$$

$$E\{\Gamma\Gamma\} \approx (2A^6 \delta^2 + A^4 \delta^4) \eta_1 u(2N_1 - d),$$

where  $d = n_1 - n_2$  (assuming  $n_1 > n_2$ ),  $u(\cdot)$  denotes the unit step function and  $\eta_1 = \frac{8}{45} N_1^5 - \frac{4}{9} d N_1^4 + \frac{2}{9} d^3 N_1^2 - \frac{1}{30} d^5$ , the MSE can be expressed by

$$\begin{aligned}
 E\{(\delta\omega)^2\} &\approx \frac{45}{8\text{SNR} \cdot N_1^5} \left[ \left( 4 + \frac{6}{\text{SNR}} \right) \right. \\
 &\quad \left. - 45 \left( 2 + \frac{1}{\text{SNR}} \right) \frac{\eta_1 \cdot u(2N_1 - d)}{4N_1^5} \right]. \tag{25}
 \end{aligned}$$

Specifically, if  $n_1 = -n_2$  with assumption of  $n_1 \geq 0$ , we have  $N_1 = N/2 - n_1$ ,  $d = 2n_1$  and  $\omega_0 = 12a_3 n_1$ . Consequently, the MSE of the  $a_3$  estimate can be derived if  $n_1 = -n_2$  and scaled by  $1/(12n_1)$ . The result is found to minimize at  $n_1 \approx 0.229N$ :

$$E\{(\delta a_3)^2\} \approx \frac{1582.5 + \frac{2829.7}{\text{SNR}}}{N^7 \text{SNR}}. \tag{26}$$

Given the asymptotic MSE of the  $a_3$  estimate, it is required to determine another time pair to estimate the  $a_4$ . The estimates of  $a_3$  and  $a_4$  can be rewritten in a compact form:

$$[\mathbf{a}] = [\boldsymbol{\rho}]^{-1} [\boldsymbol{\omega}], \tag{27}$$

where  $[\mathbf{a}] = [a_3, a_4]^T$ ,  $[\boldsymbol{\omega}] = [\omega_1, \omega_2]^T$ , and

$$\begin{aligned}
 [\boldsymbol{\rho}] &= [6(n_1 - n_2), 12(n_1^2 - n_2^2); \\
 &\quad 6(n_3 - n_4), 12(n_3^2 - n_4^2)].
 \end{aligned}$$

According to (27), the covariance matrix of  $[\mathbf{a}]$  can be determined as [10]  $\mathbf{C}_a = ([\boldsymbol{\rho}]^T [\mathbf{C}_\omega]^{-1} [\boldsymbol{\rho}])^{-1}$ , where  $\mathbf{C}_\omega$  is the covariance matrix for the generalized IFR estimate vector  $\boldsymbol{\omega}$  defined as  $[\mathbf{C}_\omega]_{ij} = E\{\delta\omega_1 \cdot \delta\omega_2\}$ .

With a tedious and straightforward deduction similar as (25),  $E\{\delta\omega_1 \cdot \delta\omega_2\}$  can be determined given  $n_3/N, n_4/N$ , and SNR. Furthermore, the variance of  $\delta a_4$  can be correspondingly determined using above results. For a given  $n_1 = -n_2 = 0.229N$ , minimum variance of the  $a_4$  estimate is obtained for  $n_3 \approx 0.276N$  and  $n_4 \approx -0.098N$ . In derivation we used MATLAB. The minimum MSE of the  $a_4$  is

$$E\{(\delta a_4)^2\} \approx \frac{41424 + \frac{87176}{\text{SNR}}}{N^9 \text{SNR}}. \tag{28}$$

#### REFERENCES

- [1] A. W. Rihaczek, "Principles of high-resolution radar," *CA: Peninsula*, 1985.
- [2] B. Porat, "Digital processing of random signals: theory and methods," *Englewood Cliffs, NJ: Prentice Hall*, 1994.
- [3] S. Peleg and B. Friedlander, "The discrete polynomial phase transform," *IEEE Trans. Signal Processing*, Vol. 43, pp. 1901-1914, Aug. 1995.
- [4] D. C. Reid, A. M. Zoubir, and B. Boashash, "Air-craft flight parameter estimation based on passive acoustic techniques using the polynomial Wigner-Ville distribution," *J. Acoust. Soc. Amer.*, Vol. 102, pp. 207-223, 1997.

- [5] T. Abotzoglou, "Fast maximum likelihood joint estimation of frequency and frequency rate," *IEEE Trans. on Aerosp. Electron. Syst.*, Vol. AES-22, pp. 708-715, Nov. 1986.
- [6] S. Golden and B. Friedlander, "A modification of the discrete polynomial transform," *IEEE Trans. Signal Processing*, Vol. 46, pp. 1452-1455, May. 1998
- [7] B. Porat and B. Friedlander, "Asymptotic statistical analysis of the high-order ambiguity function for parameter estimation of polynomial-phase signals," *IEEE Trans. Inform. Theory*, Vol. 42, pp. 995-1001, March 1996.
- [8] B. Barkat and B. Boashash, "Design of higher order polynomial Wigner-Ville distributions," *IEEE Trans. Signal Processing*, Vol. 47, pp. 2608-2611, 1999.
- [9] P. O'Shea, "A new technique for estimating instantaneous frequency rate," *IEEE Signal Processing Lett.*, Vol. 9, pp. 251-252, Aug. 2002.
- [10] P. O'Shea, "A fast algorithm for estimating the parameters of a quadratic FM signal," *IEEE Trans. Signal Processing*, Vol. 52, pp. 385-393, Feb. 2004.
- [11] M. R. Spiegel, "Schaum's Mathematical Handbook of Formulas and Tables," *McGraw-Hill*, 1998.
- [12] S. Barbarossa, A. Scaglione, and G. Giannakis, "Product high-order ambiguity function for multi-component polynomial phase signal modeling," *IEEE Trans. Signal Processing*, Vol. 48, pp. 691-708, Mar. 1998.
- [13] P. Wang and J. Yang, "Multicomponent chirp signals analysis using product cubic phase function," *Digital Signal Processing: A Review Journal*, Vol. 16, pp. 654-669, Nov. 2006.
- [14] P. Wang, J. Yang and I. Djurović, "Algorithm extension of cubic phase function for estimating quadratic FM signal," *Proc. of the 32nd International Conference on Acoustics, Speech, and Signal Processing (ICASSP'2007)*, Hawaii, USA, Vol III, pp. 1125-1128, April 2007.
- [15] C. Ioana and A. Quinquis, "Time-frequency analysis using warped-based high-order phase modeling," *EURASIP Journal on Applied Signal Processing*, Vol. 17, pp. 2856-2873, 2005.
- [16] S. Peleg and B. Porat, "Linear FM signal parameter estimation from discrete-time observations," *IEEE Trans. Aerosp. Electron. Syst.*, Vol. 27, pp. 607-614, July 1991.
- [17] B. Ristic and B. Boashash, "Comments on "The Cramer-Rao Lower Bounds for Signals with Constant Amplitude and Polynomial Phase", " *IEEE Trans. Signal Processing*, Vol. 46, pp. 1708-1709, June 1998.
- [18] S. M. Kay, "Fundamental of Statistical Signal Processing: Estimation Theory," *Upper Saddle River, NJ: Prentice Hall*, 1998.